Florence, Italy 12-16 July 2015
ICSV22
The 22nd International Congress on Sound and Vibration

ACOUSTIC RESONANCE FREQUENCIES OF AN OPEN CAVITY WITH NON-SYMMETRIC AND NON-PARALLEL WALLS

Cristobal Gonzalez Diaz and Pedro Cobo Parra

Instituto de Tecnologias Fisicas y de la Informacion (ITEFI),
Consejo Superior de Investigaciones Cientificas (CSIC),
Serrano, 144, 28006, Madrid (Spain)
e-mail: cristobal.g.diaz@csic.es

When airflow passes over an open cavity, due to vortex shedding at the upstream edge of the cavity and the geometry or shape of the cavity, high-level aero-acoustic noise may be generated. When the incident acoustic waves produced by the airflow couples with the acoustic cavity resonance frequencies intensive tones are generated in and around the cavity at resonant discrete frequencies. Cavity noise is one of the most important airframe noises. Sound radiation due to the acoustic cavity resonances in an open cavity could be achieved by changing its geometry or shape. This paper presents simulated results, using Finite Element Methods, of the influence in the resonance frequencies of an open cavity with non-symmetric and non-parallel walls. Different parameters of the open cavity, such as the angle between the walls of the open cavity will be considered to optimise its geometry.

1. Introduction

The interaction of flow with an open cavity is of certain interest both in aeroacoustics and noise control [1, 2]. Airframe noises are generated by the interaction between the vortex streets in the turbulent wake or between the vortices and the solid body edge(s). The phenomena are further complicated by a possible aero-acoustic feedback loop or a possible Helmholtz fluid resonance. Thus, the main consequence of the flow over the open cavity is the generation of cavity noise [3]. Cavity noise is one of the most important airframe noises [2, 3]. When flow passes over a cavity or opening, due to vortex shedding at the upstream edge of the cavity, intensive tone noises may be generated. Strong tonal oscillations occur in a feedback loop between the two edges of the cavity opening. First, the vortices generated and shed from the upstream edge of the cavity convect downstream, impinge on the other edge, and produce acoustic waves. Then, as the acoustic waves propagate either inside or outside of the cavity to the upstream edge, where receptivity of the wall jet shear layer is high, a new instability wave (vortex) is stimulated and shed, a feedback cycle is thus completed. The tone noise generated in this way may be categorized as fluid-dynamic oscillation noise. Most high-speed flow (supersonic, transonic, or high subsonic flows) noises are generated by the fluid dynamic feedback oscillation mode. However, at low flow speed [2], depending on the geometry of the cavity, another type of tone noise due to fluid resonant oscillation within the cavity may occur. The sound waves inside the cavity may be longitudinal or transverse depending on the

aspect ratio of the cavity. For a deep cavity at low flow speed, both major tone noise-generating mechanisms may coexist. If one or more walls of a cavity undergo displacement that is large enough to exert feedback control on the shear layer perturbations during the cavity oscillation, the excitation is defined as fluid elastic. The vibrating structure has the same function as the resonating wave in a fluid resonant oscillation. A resonant type process is used to amplify the perturbed shear layer flow. Wheel wells and Auxiliary Power Unit compartments during the airplane landing and take off operations, the bogie section and the shallow cavity accommodating the pantograph of a high speed train, or the open sunroofs and open windows of a car driven at high speed are sources of high level cavity tones. Several researches have reported numerical methods to provide the eigenvalues (resonances frequencies) and eigenfunctions (normal modes) of open cavities without flow. Koch [4] proposed to find the acoustic resonances of 2D and 3D rectangular open cavities by solving Helmholtz wave equation by finite-element methods (FEM). Ortiz et al. [5] suggested the use of the Image Source Model (ISM) to obtain the impulse response of an open cavity. This method gives the acoustic resonances of a 3D open cavity by a fast and efficient method, which models the time response at any point in the medium as the convolution of the source waveform with the impulse response of the cavity.

The acoustic resonances in the open cavity can be attenuated by noise control techniques. One passive control technique consists of lining the inner walls of the cavity with absorbing material [6, 7]. Whilst porous materials provide wideband absorption, they are discouraged in presence of airflow. Since open cavity tones are usually driven by air flow (wheel wells in airplanes, shallow cavity above bogies in trains, sunroof in cars), alternative absorbers supporting air flowing might be used. Micro-Perforated Panels (MPP) are recognized as the next generation absorbing materials. Furthermore, they can be used in presence of air flow [8].

Other passive control technique to attenuate the acoustic resonances of an open cavity is to change its geometry. In general, the design modification of an open cavity to decrease the sound it produces enforces design requirements limits to the design freedom. Overall open cavity dimensions are restricted due to operation of the plane (the limitation of runway loads defines number of wheels and spacing, gear locations defined by lateral stability and rotation before lift-off, brake cooling system), safety (tyre burst) and cost (weight, system complexity, maintenance). Therefore few constrains should be taking into account such as the volume, length, width, depth... of an open cavity where the landing gear should fit.

The major aim of this work is to report the influence in the resonance frequencies of an open cavity with non-symmetric and non-parallel walls. The geometry of the open cavity used in this study will be described in Section 2. The numerical procedure – Finite Elements Analysis (FEM) used and the numerical results will be presented in Section 3 and Section 4 respectively. Finally, the main conclusions will be disclosed in Section 5.

2. The open Cavity – Geometry

A cavity with non-parallel lateral walls and depth D, open at the topside is considered in this paper. The floor and opening of the cavity are rectangular with dimensions (L_b, W_b) and (L_t, W_t) respectively, see Figure 1. The inner dimensions of the open cavity with parallels and symmetric wall are (W, L, D) = (53, 32, 38) cm, in such case $L_b = L_t = L$ and $W_b = W_t = W$.

A three-dimensional Cartesian coordinate system (X, Y, Z) with the origin at the center of the cavity is also shown in Figure 1. The front (w_1) and rear (w_3) walls subtend an angle α_1 and α_3 respectively with the floor of the cavity, and the lateral walls (w_1 and w_4) form an angle α_2 and α_4 respectively with the floor of the cavity. A point source S is positioned at the front wall (w_1) of the cavity, with coordinates (x_S, y_S, z_S) = (-0.195, -0.16+slope_w_1, 0.1) m, where slope_w_1 depends on the inclination of the w_1, in such a way the point source is always located on the front wall (w_1). The problem consists of calculating the sound signal at the receivers R_n, with coordinates

(x_{Rn}, y_{Rn}, z_{Rn}). A baffle is situated around the open wall of the cavity in order to avoid back radiation between the source and the measurement points. The sound signal have been simulated in four points; R_1; a lower point close to the floor and opposite wall containing the point source, R_2; a middle point set close to the lateral wall (w_4) and finally two points located outside the cavity, R_3: a point above the upper baffle opposite to the wall containing point source and R_4: a point also above the upper baffle close to the lateral wall (w_4) farther away from the point source. Table 1 and Figure 2 summarises the coordinates of the points.

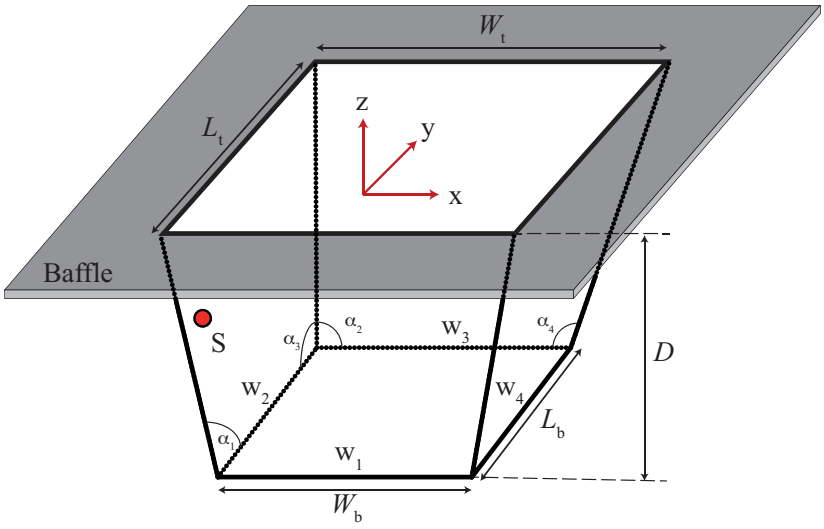

Figure 1. Open cavity with non-parallel walls.

Table 1. Coordinates of the source and receiver points.

Points	X(m)	Y(m)	Z(m)
Source	-0.195	-0.16+slope_w1	0.1
Receiver R_1	0.135	0.11	-0.17
Receiver R_2	0.215	0.11	0.13
Receiver R_3	0.135	0.21	0.21
Receiver R_4	0.335	0.16	0.21

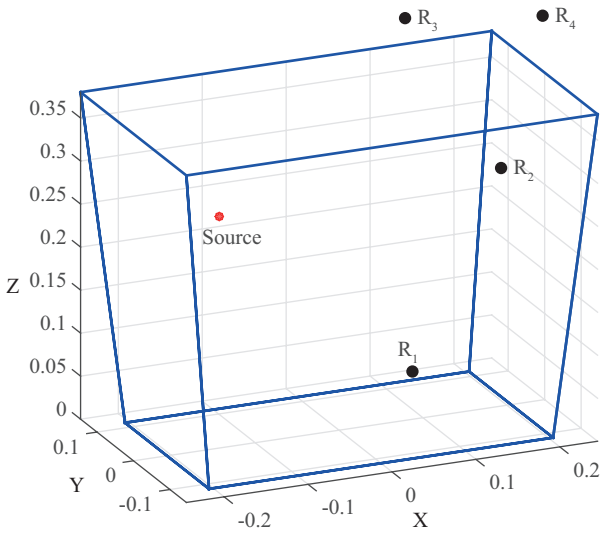

Figure 2. Source and Receiver (R_1, R_2, R_3 and R_4) positions.

3. Numerical procedure – Finite Elements Analysis (FEM)

The Finite Element Method (FEM) software used in this work is Comsol Multiphysics 5.0. The numerical model is experimentally validated by comparing the measured natural frequencies [5] to the simulated natural frequencies extracted from the peaks of the Frequency Response Functions (FRF) when the open cavity has symmetric and parallel walls ($L_b = L_t = L$ and $W_b = W_t = W$). Table 2 shows the modal frequencies of the open cavity extracted from the peaks of FRF; experimentally and simulated. The selected mesh size of the model results in an acceptable balance between the frequency range of interest and the calculation time. The computational cost increases rapidly with frequency. In the performed simulation a Monopole Point Source located in the "Source Point" excites the cavity. A frequency resolution of 1 Hz and frequency range of 1-1000 Hz are chosen for the frequency domain simulations. The significant peaks of this FRF were identified as the acoustic resonance frequencies of the cavity.

Table 2. Modal frequencies of the symmetric and with parallel walls extracted from the peaks of the FRF [5].

Mode	F_{exp} (Hz)	F_{num} (Hz)
(0,0,0)	157	159
(1,0,0)	374.4	368
(0,1,0)	575	569
(2,0,0)	680.9	673
(2,1,0)	863.4	863
(0,2,0)	1103	1091
(2,2,0)	1290	1269

A Perfectly Matched Layer (PML) has been chosen to simulate the presence of an open boundary and the radiation of energy to the infinity, this layer absorbs all outgoing wave energy in frequency-domain problems without any impedance mismatch—causing spurious reflections—at the boundary [9].

4. Results

Assuming a Cartesian coordinates system with origin at the centre of the cavity (see Figure 1 for further details), the source is located at $(x_s, y_s, z_s) = (-0.195, -0.16, 0.1)$. The impulse responses were measured at 4 receiver points inside and outside the cavity (Table 1 and Figure 2) for six different geometry configurations.

1. Configuration 1: the cavity has symmetric and parallel walls ($L_b = L_t = L$ and $W_b = W_t = W$), and $\alpha_{1\text{-}4} = 0$, that is, a rectangular cavity.
2. Configuration 2: in this case the front (w_1) and rear (w_3) walls are parallel, however the angles between both walls and the floor is not equal to zero, instead $\alpha_2 = -\alpha_4 \neq 0$. The lateral walls ($w_2$ and w_4) are not parallels and $L_b < L_t$ and both α_1 and α_3 are positive.
3. Configuration 3: in this case all the angles between the walls and the floor are positives but not equal ($\alpha_{1\text{-}4} > 0$ and $\alpha_1 \neq \alpha_2 \neq \alpha_3 \neq \alpha_4$) therefore $L_b < L_t$ and $W_b < W_t$.
4. Configuration 4: in this configurations the angle between the walls and the floor are positive but one ($\alpha_{1\text{-}3} > 0$ and $\alpha_4 < 0$). Also $L_b < L_t$ and $W_b < W_t$.
5. Configuration 5: in this case the angle between the walls and floor are equal and negative ($\alpha_1 = \alpha_2 = \alpha_3 = \alpha_4 < 0$), hence $L_b > L_t$ and $W_b < W_t$.
6. Configuration 6: in this case the angle between the walls and floor are also equal but in this case positive ($\alpha_1 = \alpha_2 = \alpha_3 = \alpha_4 > 0$), hence $L_b < L_t$ and $W_b < W_t$.

Figure 3 shows the frequency response function between the source and the receiver R_1, which is located close to the floor of the cavity and opposite wall w_1, which contains the point source. In this paper the absorption coefficient of the cavity walls has been assumed as "Hard Boundary Walls", therefore the simulations tend to show sharp peaks. It can be seen that by changing the geometry of the cavity the resonance frequencies of the cavity are attenuated. It can also be observed that at high frequencies, where the passive strategies are more efficient, the attenuation is higher. The resonance frequencies are also shifted as the geometry is changed that is due to the fact that the volume of the cavity is not constant. The influence is higher inside the cavity (Figure 3 and 4) that outside the cavity (Figure 5 and 6), that is due to the fact that the point are located closer to the source, therefore the influence is of the geometry configuration is higher.

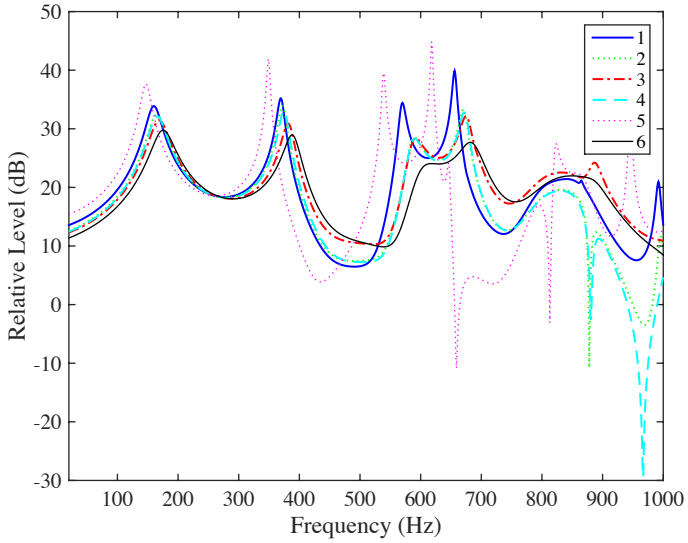

Figure 3. Simulated FRF at the **Receiver R_1** for different geometry configurations. Blue and solid line = configuration 1, green and dotted line = configuration 2, red and dashdot line = configuration 3, cyan and dashed line = configuration 4, magenta and dotted faint line = configuration 5 and black and solid faint line = configuration 6.

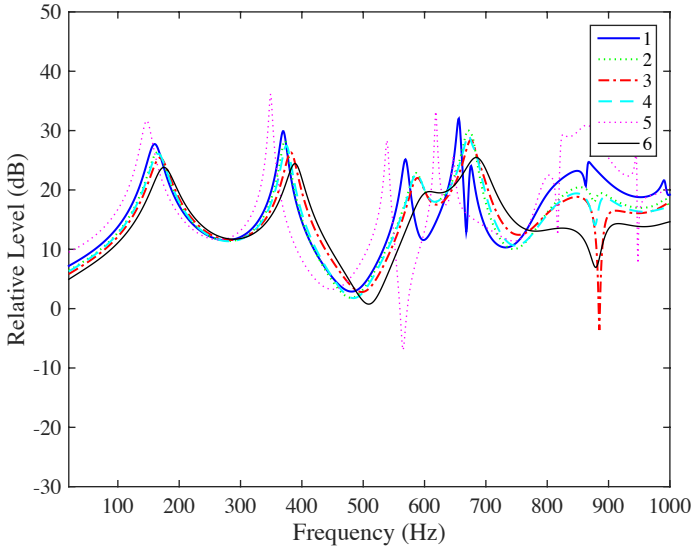

Figure 4. Simulated FRF at the **Receiver R_2** for different geometry configurations. Blue and solid line = configuration 1, green and dotted line = configuration 2, red and dashdot line = configuration 3, cyan and dashed line = configuration 4, magenta and dotted faint line = configuration 5 and black and solid faint line = configuration 6.

Figure 4 shows the frequency response function between the source and the receiver R_2, which is set in the upper middle part of the cavity close to the lateral wall (w_4) further away from the source.

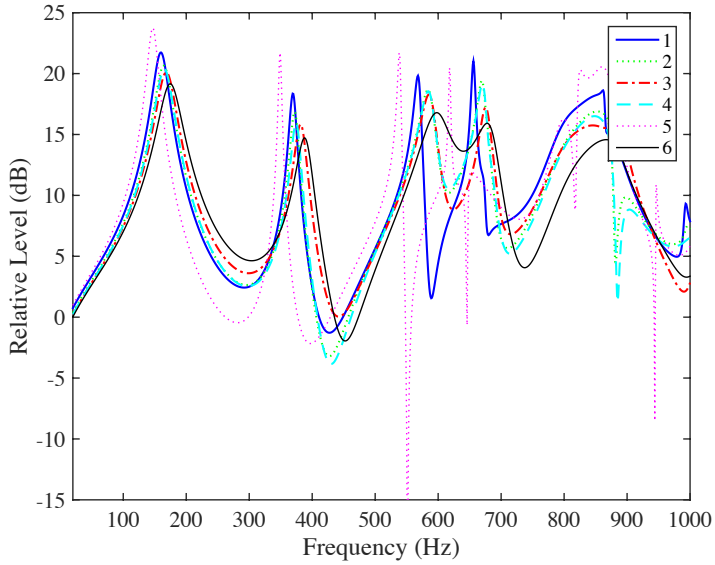

Figure 5. Simulated FRF at the **Receiver R_3** for different geometry configurations. Blue and solid line = configuration 1, green and dotted line = configuration 2, red and dashdot line = configuration 3, cyan and dashed line = configuration 4, magenta and dotted faint line = configuration 5 and black and solid faint line = configuration 6.

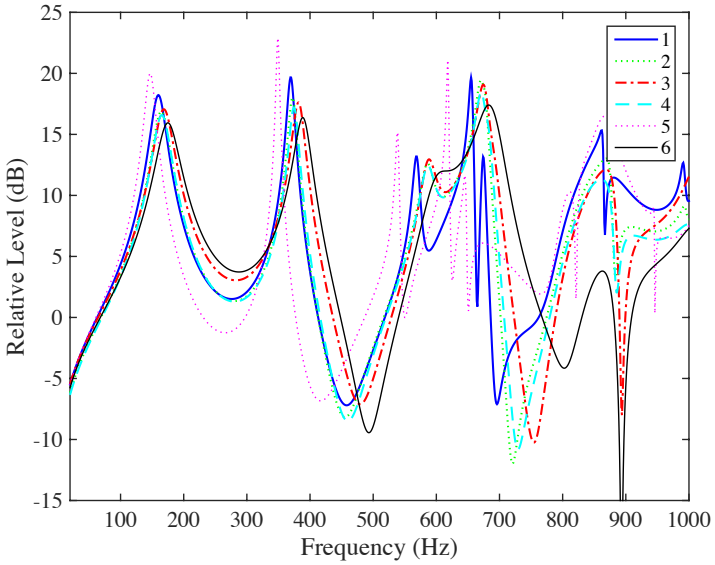

Figure 6. Simulated FRF at the **Receiver R_4** for different geometry configurations. Blue and solid line = configuration 1, green and dotted line = configuration 2, red and dashdot line = configuration 3, cyan and dashed line = configuration 4, magenta and dotted faint line = configuration 5 and black and solid faint line = configuration 6.

Figure 5 and 6 show the frequency response function between the source and the receiver $R_{3,4}$, which are both set outside the cavity above the baffle: R_4 opposite to the wall (w_3) containing the point source and R_4 close to the lateral wall (w_4). As already pointed out previously, the influence of changing the geometry of the cavity affects less in these points situated outside (Figure 5 and 6) the cavity that to those situated inside (Figure 3 and 4) the cavity. These points are farther away

from the source point. However the peaks are also decreased. As expected, the configuration 5 seems to be the less suitable among all the configurations presented in this paper. This is the configuration with walls inclined toward the interior, like a pyramid with a truncate top. Also the configuration 6 seems the best in term of attenuation of the resonance frequencies, however it might not be the more practical in term of geometry.

5. Summary and Conclusions

The influence in the amplitude of the resonance frequencies of an open cavity with non-symmetric and non-parallel walls has been considered in this paper.

The Frequency Response Function between four receiver points, two located inside and two outside the cavity have been presented for six different geometry configurations.

It has been shown than changing the geometry of the cavity modifies the resonance frequencies of it. It has also been observed that at high frequencies, where the passive strategies are more efficient, the attenuation is larger and the influence is higher inside the cavity that outside the cavity.

Acknowledgments

The research leading to these results has received funding from the EU Seventh Framework Programme Marie Curie IEF project "ACOCTIA" (FP7-PEOPLE-2011-IEF, Grant Agreement No. 301287).

REFERENCES

1. H.E. Plumblee, J.S. Gibson, L.W. Lassiter, A theoretical and experimental investigation of the acoustic response of cavities in aerodynamic flow, in: Technical Report No. WADD-TR-62-75, Air Force Rep., U.S., 1962.
2. J.E. Rossiter, Wind-tunnel experiments on the flow over rectangular cavities at subsonic and transonic speeds, Aeronautical Research Council Reports and Memoranda, Technical report 3438, (1964).
3. X. Gloerfelt, Cavity Noise, in: VKI Lectures: Aerodynamic noise from wall-bounded flows, Von Karman Institute, 2009.
4. W. Koch, Acoustic Resonances in Rectangular Open Cavities, AIAA Journal, 43 (2005) 2342-2349.
5. S. Ortiz, C.L. Plenier, P. Cobo, Efficient modeling and experimental validation of acoustic resonances in three-dimensional rectangular open cavities, Applied Acoustics, 74 (2013) 949-957.
6. S. Ortiz, C. Gonzalez Diaz, P. Cobo, F. Montero de Espinosa, Attenuating open cavity tones by lining its walls with microperforated panels, Noise Control Engineering Journal, 62 (2014) 145-151.
7. C. Gonzales Diaz, S. Ortiz, P. Cobo, Attenuation of acoustic resonances in an inclined open cavity using Micro Perforated Panels, in: 43rd International Congress on Noise Control Engineering, The Australian Acoustical Society, PO Box 1843, Toowong DC QLD 4066, AUSTRALIA, Melbourne, Australia, 2014.
8. P. Cobo, H. Ruiz, J. Alvarez, Double-Layer Microperforated Panel/Porous Absorber as Liner for Anechoic Closing of the Test Section in Wind Tunnels, Acta Acustica united with Acustica, 96 (2010) 914-922.

9. J.-P. Berenger, A perfectly matched layer for the absorption of electromagnetic waves, Journal of Computational Physics, 114 (1994) 185-200.